Effect of Baffle Design on the Off-bottom Suspension Characteristics of Axial-flow Impellers in a Pilot-scale Mixing Vessel

M. Špidla*, V. Sinevič, and V. Machoň
Department of Chemical Engineering, Institute of Chemical Technology
Technická 3, 166 28 Prague 6, Czech Republic

Original scientific paper
Received: January 21, 2005
Accepted: October 1, 2005

The work aimed to determine the optimum system parameters for complete particle suspension. The experiments performed in a pilot-scale vessel (D = 1 m) were focussed on a study of the effects of geometrical vessel arrangements and, above all, on the effect of alterations to the shape of the baffles.

The experiments sought above all to determine the critical impeller speed, n_{cr}, and impeller power consumption, P, in a vessel equipped with non-standard, arrow-headed baffles, and also to compare these experimental data with results arising from measurements undertaken in the same vessel, but equipped with four standard straight baffles. Three types of axial-flow impellers were investigated, each of them in two sizes. The suspension volume fraction, φ, varied up to 10 %, with particle diameter from 0.1 to 3 mm.

The results aid the selection of the most favourable types of baffles and impeller giving the minimum power consumption and/or the minimum speed for just-suspended particles. It is shown that the installation of arrow-headed baffles appears to be energetically more advantageous compared with the standard baffling.

Keywords:
Mixing, solids suspension, non-standard baffles, critical impeller speed, power consumption, pilot-scale mixing vessel

Introduction

Suspending solid particles in a low-viscosity liquid is one of the most widespread operations in chemical and biochemical industries. Complete lifting of the solid phase and its dispersion in liquid is feasible at a certain value of the axial component of liquid velocity in the system. The required axial flow pattern of a solid-liquid phase is produced by using the appropriate impeller type in a vessel equipped with baffles, whose primary purpose is not only to convert swirling motion into the preferred axial flow, but also to suppress the central vortex formation and to increase the power input. The discharge axial flow produced by the impeller impinges on the vessel base, flows radially to the vessel wall, then up the wall, lifting up the settled particles, and then returning to the impeller from above.

The state of complete suspension, which is closely related to the critical impeller speed, n_{cr}, is usually determined using the Zweitering[1] criterion, at which none of the solid particles remain stationary on the vessel bottom for longer periods than 1 – 2 s. Generally, the minimum impeller speed, n_{cr}, is a complex function of the impeller type, physical properties of solids and liquid, solids loading, system geometry, and scale.[2–8]

Many agitated vessels use standard baffling, which comprises four flat vertical plates, radially directed, and spaced at 90° intervals around the vessel periphery, and running the length of the vessel's straight side. The standard baffle width is D/10 or D/12.

There are many instances in which a non-standard baffling is commonly used.[9] The influence of the distance between the lower edge of the flat baffle and the vessel bottom on the impeller power consumption and/or on the critical impeller speed was studied experimentally.[10–14] *Karcz* and *Major*[15] investigated the influence of tubular baffles spaced with and without gap at the vessel wall on the power consumption. In these works, positive effects were found and quantified when non-standard baffles were used. Other non-standard profiled shapes of baffles were also mentioned,[9] such as triangular, semicircular or elliptical in cross-section. Recently *Medek* and *Seichter*[16] presented the basic hydrodynamic characteristics for a vessel equipped with four double-convex baffles. A remarkable increase from 13 % to 39 % in the impeller flow rate numbers, q_N, was found for all the types of axial-flow

* Corresponding author. Tel.: +420-2-20443233; fax: +420-2-3333 7335.
E-mail address: Michal.Spidla@vscht.cz.

impellers used, in comparison to the standard vessel baffling. Hereafter, this type of non-standard baffling is referred to as arrow-headed baffles (AH-B) in the present work.

The purpose of this paper is to present the experimental hydrodynamic characteristics that are of relevance in the field of suspension mixing in vessels with such non-standard, arrow-headed baffles. The experimental endeavour was directed at determining the critical impeller speed, n_{cr}, and at ascertaining the impeller power requirements at n_{cr}. One set of experiments was performed in a vessel fitted with four standard baffles (ST-B), the second one was carried out in the same vessel, but fitted with four AH-Bs. A further task was to compare the advantages of AH-Bs with the standard ones from the point of view of the impeller suspension efficiency, π_S.

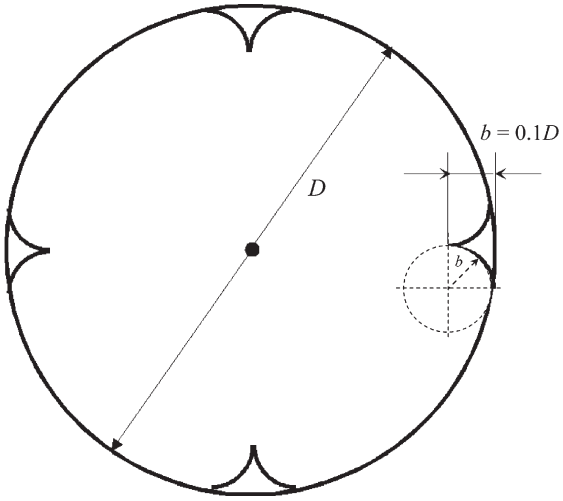

F i g . 2 – *Cross-section of the mixing vessel equipped with the arrow-headed baffles (AH-B)*

Experimental set-up

Experiments were carried out in a flat-bottomed, cylindrical, clear Plexiglas, pilot-scale tank of diameter D = 1 m, equipped with four ST-Bs of width b = 0.1 D, filling height $H = D$. Figure 1 renders the main geometrical parameters of the mixing vessel.

The sketch of the arrow-headed baffles is in Fig. 2. The baffles are of an uncomplicated structure of high rigidity, inhibiting baffle oscillations and thus formation of additive eddies. An even simpler structure can also be used, with AH-Bs having a triangular cross-section.

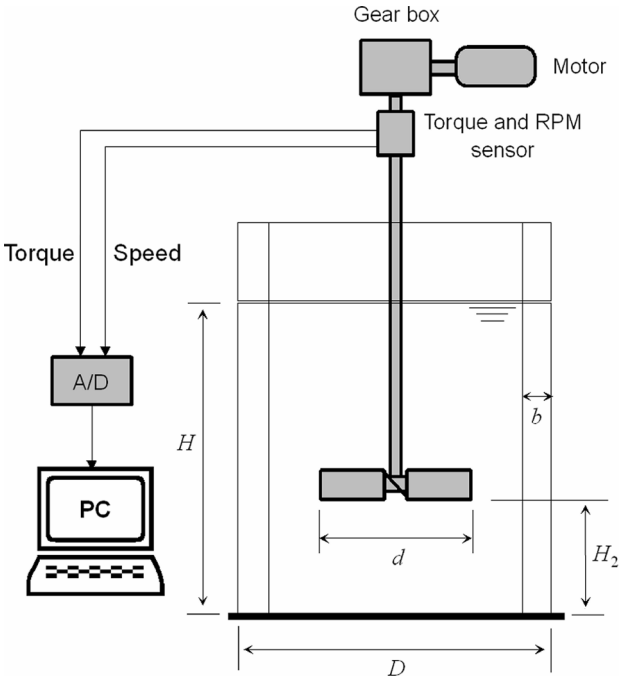

F i g . 1 – *Experimental set-up with geometrical parameters of the mixing vessel*

The suspension of classified ballotini in tap water was used as a model suspension, at volumetric fraction φ_V = 2.5, 5, 7.5 and 10 %. The mean particle diameters were d_p = 0.14; 0.35; 0.82; 1.32 and 3.02 mm, at densities ρ_p = 2478; 2500; 2539; 2507 and 2530 kg m^{-3}, respectively. Flat six pitched-blade impellers (pitch 45°, blade width h = 0.2 d), and two hydrofoil impellers Lightnin A315 and Techmix 335 (see Fig. 3), operating in the

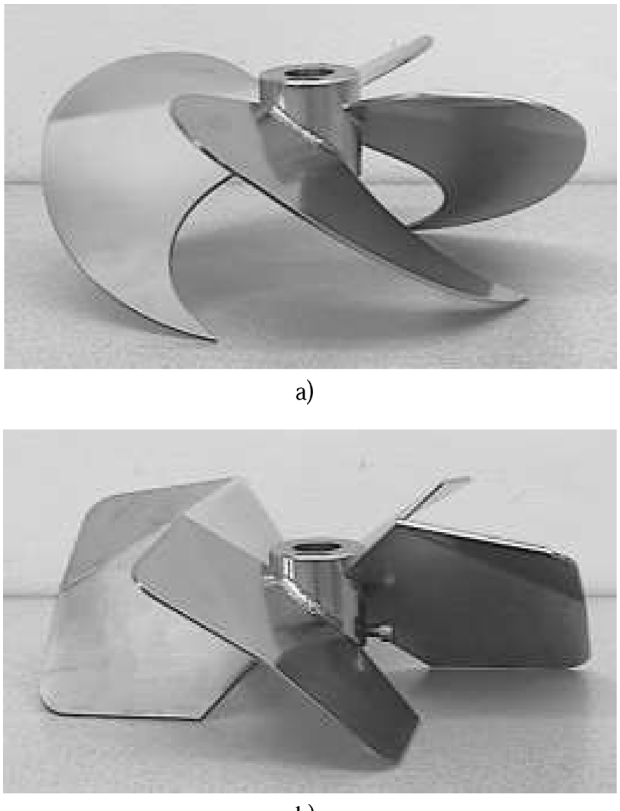

a)

b)

F i g . 3 – *Hydrofoil impellers: a) Techmix 335, b) Lightnin A315*

Table 1 – *Symbols and main geometrical parameters of the impellers*

Impeller type	Symbol	Impeller diameter d/m	D/d	Number of blades N_B	Other specification
Flat six pitched-blade turbine	B6	0.333	3	6	$\alpha = 45°$
	C6	0.400	2.5	6	$h = 0.2\ d$
Techmix 335	TXB	0.333	3	4	main angle $\alpha = 35°$
	TXC	0.400	2.5	4	falcate shape of blades
Lightnin A315	LNB	0.343	3	4	main angle $\alpha = 40°$
	LNC	0.400	2.5	4	$h = 0.56\ d$

down pumping mode, were used in the suspension experiments. The vessel-to-impeller diameter ratios were D/d = 2.5 and 3, and the impeller off-bottom clearance was $H_2 = d$. Major geometrical and structural parameters, as well as the impeller symbols for all the impellers, are shown in Table 1.

The impeller shaft was driven by a servo-controlled variable-speed DC motor by means of a V-belt and a pulley, and the impeller speed was measured using an opto-electronic disk system coupled to a digital counter. A calibrated strain-gauge bridge mounted on a torsion rod was employed for torque measurements, wherein the output bridge signal was transmitted by telemetry and digitised for the PC data processing.

The critical impeller speed, n_{cr}, was determined from the course of the power number characteristic Po (n).[17] A detailed treatise describing this experimental method was presented in a previous paper.[18] In this way, the values of n_{cr} match very well with those obtained by simultaneous visual observations (max. ±5 %).

Evaluation of suspension characteristics

The theoretical outlines for suspension of solid particles, as well as an overview of the appropriate experimental techniques for the assessment and identification of the state of particle suspension, are presented e.g. by *Rieger* and *Ditl*,[19] who introduced a modified Froude number, Fr', which is a function of relative particle size, d_p/D, and volume fraction of suspension, φ, so that $Fr' = f\,(d_p/D;\ \varphi)$.

Subsequent papers[20–23] were devoted to effects of the relative particle diameter d_p/D and of suspension concentration, φ, on the values of Fr'.

The relation $Fr' = f\,(d_p/D;\ \varphi)$ has been generalized[22] in the functional form

$$Fr' = \frac{C_{41}\mathrm{e}^{c_{42}\varphi}\left(\frac{d_p}{D}\right)^{a_1+a_2\varphi}}{\left\{1+\left[C_{31}\mathrm{e}^{c_{32}\varphi}\left(\frac{d_p}{D}\right)^{c_1+c_2\varphi}\right]^{10}\right\}^{\frac{1}{10}}} \qquad (1)$$

where the values of coefficients C_{41}, C_{42}, C_{31}, C_{32}, a_1, a_2, c_1 and c_2, evaluated by regression analysis, are different for individual impeller types.

In this paper, the relation $Fr' = f\,(d_p/D;\ \varphi)$ according to Eq. (1) was used in data evaluations for ST-B as well as for AH-B. A good adequacy of experimental and calculated values of $Fr' = f\,(d_p/D;\ \varphi)$ is illustrated, e.g. for the impeller B6, in Fig. 4.

For mutual comparisons of suspension efficiency for different types of impellers, *Rieger*[24] introduced an impeller suspension efficiency π_S as follows

$$\pi_S = Po\sqrt{Fr'^3\left(\frac{d}{D}\right)^7} \qquad (2)$$

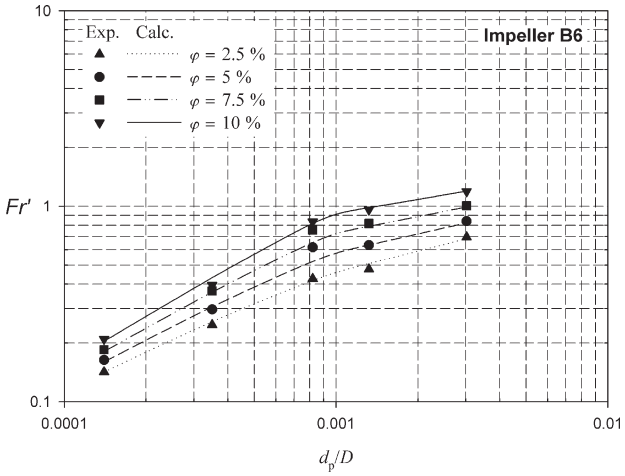

Fig. 4 – *Comparison of experimental and calculated values of Fr′ for the impeller B6 with AH-B*

where *Po* is the power number at just-suspended conditions. The geometrical arrangement of mixing equipment with the lowest values of π_S determines the most appropriate system from an energy-saving aspect, see Eq. (3), which is obtained after substitutions for *Po* and *Fr′* into Eq. (2)

$$\pi_S = \frac{P}{\rho_S}\sqrt{\left(\frac{\rho}{g\Delta\rho}\right)^3 \frac{1}{D^7}} \qquad (3)$$

Further, at *Po* = constant in the turbulent flow region, the general functional dependence $\pi_S = f(d_p/D; \varphi)$ follows from Eq. (2).

From known values of $\pi_S = f(d_p/D; \varphi)$ of individual impellers, physical properties of the suspension, and vessel diameter *D,* the volumetric impeller power $P_m \equiv P/V$ at just-suspended conditions can be calculated from Eq. (3). Consequently, the impeller power P_m is proportional to the dimensionless quantity π_S. This method can also be found in other papers by *Špidla* et al.[25,26]

Results and discussion

Power numbers Po_0 in water and *Po* in just-suspended suspensions

Comparisons of the values Po_0 and *Po* with the standard baffles and with the arrow-headed ones are shown in Fig. 5, and the values are summarised in Table 2. For a given impeller, the *Po* value is reported as an average of the values obtained for all the concentrations and particle diameters at the just-suspended state. For these average values, the relative standard deviations ranged from 2 to 5 % and from 4 to 12 % for AH-B and ST-B, respectively. The arrow-headed baffles decrease both Po_0 and *Po* values about 12 % on the average compared with the standard baffles, see Table 2. This systematic decrease indicates a better-ordered hydrodynamic flow pattern in the vessel equipped with AH-B. The highest decreases of *Po* and Po_0 were achieved when using the Lightnin A315 impeller.

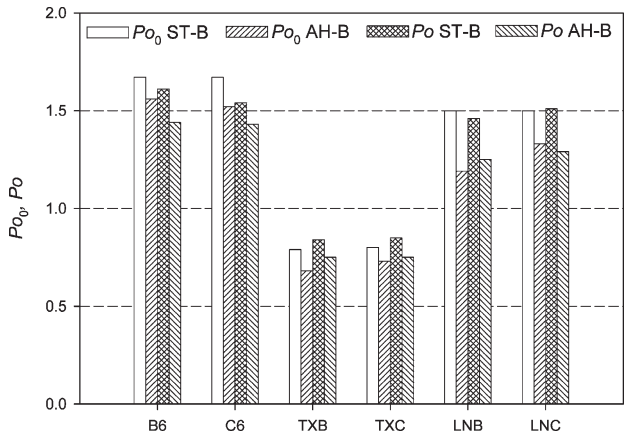

Fig. 5 – *Comparison of the impeller power number in water, Po_0, and in a suspension (just-suspended), Po, for ST-B and AH-B, H_2/d = 1*

Table 2 – *Power numbers in water Po_0 and in just-suspended suspensions Po in the vessel with ST-B and AH-B, H_2/d = 1*

Impeller symbol	D/d	Po_0		δ_{r,Po_0} [1]	Po		$\delta_{r,Po}$ [1]
		ST-B	AH-B	%	ST-B	AH-B	%
B6	3	1.67	1.56	−7	1.61	1.44	−11
C6	2.5	1.67	1.52	−9	1.54	1.43	−7
TXB	3	0.79	0.68	−14	0.84	0.75	−11
TXC	2.5	0.80	0.73	−9	0.85	0.75	−12
LNB	3	1.50	1.19	−21	1.46	1.25	−14
LNC	2.5	1.50	1.33	−11	1.51	1.29	−15

[1] The relative difference δ_r for quantity X is defined as $\delta_{r,X} = (X_{AH-B} - X_{ST-B})/X_{ST-B}$

A more detailed inspection of Fig. 5 shows that, whilst for hydrofoil impellers the values *Po* for both ST-B and AH-B are practically the same within the range of experimental error as the value Po_0 in water, whereas in cases of impellers B6 and C6 with narrower blades, the *Po* values are systematically about 6 % lower than Po_0.

Effects of arrow-head baffles on the critical impeller speed n_{cr}

The effect of AH-B on the modified Froude number $Fr' = n_{cr}^2\, d\rho/(\Delta\rho g)$ is shown in Fig. 6. The functions $Fr' = f(d_p/D; \varphi)$ were obtained using the evaluation method outlined in the previous section, with the coefficients of Eq. (1) summarised in Tables 3 and 4 for ST-B and AH-B, respectively. For the whole data set, the average deviation of calculated and experimental values *Fr′* does not exceed 8 %. In spite of this, it is not recommended to use these correlations in situations far removed from the investigated ranges of particle-to-vessel diameter ratio d_p/D and solids volume fractions φ.

With smaller impellers (B6, TXB, LNB with D/d = 3), the effect of the AH-B installation is relatively small. For all these impellers, the typical illustration of this effect is in Fig. 6a.

With larger impellers (C6, TXC, LNC with D/d = 2.5), the influence of different baffle types becomes more pronounced. The tips of the impeller

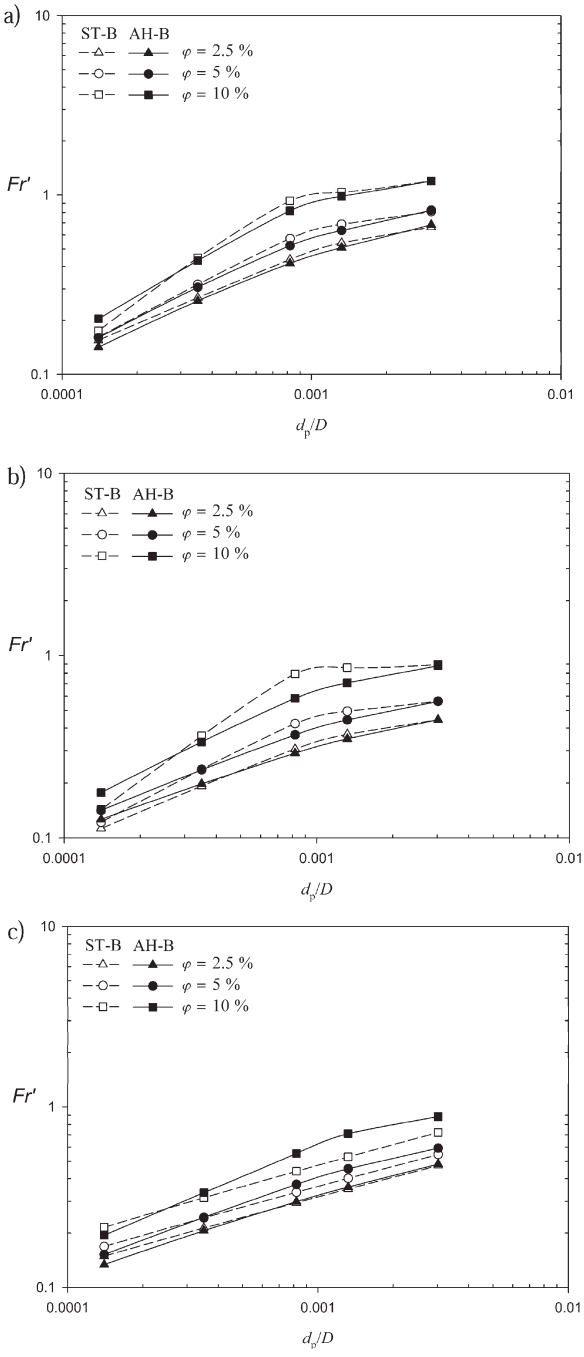

F i g . 6 – *Comparison of the functions Fr′ = f(d$_p$/D; φ) for AH-B and ST-B: a) impeller B6, b) impeller C6, and c) impeller LNC*

blades are nearer to the baffles, whose influence on the flow emanating from the impeller is more substantial. With impeller C6 in the region of $d_p/D > 3.5 \times 10^{-4}$, a lower critical impeller speed, n_{cr}, is achieved with AH-B, as depicted in Fig. 6b, whereas in the same region, it is just the other way round for the hydrofoil impellers. Figure 6c illustrates this effect in case of the Lightnin A315 (LNC) impeller.

With the hydrofoil impellers, the critical speeds are higher in the case of AH-B than of ST-B. The blades are larger and especially wider than the blades for six pitched blade turbines. Therefore, the radial velocity component of the liquid emanating from a hydrofoil impeller is higher as well. Upon installation of AH-B, the tangential and partially the radial component of the liquid motion are returned to the main liquid flow in the vessel. As a consequence of these effects, the rising axial flow of liquid along the mixing vessel wall is suppressed. Agitated suspension is largely maintained in the region under the impeller, and the lifting of the solid phase by AH-B occurs at higher critical impeller speeds.

With the six pitched-blade impeller C6, the blade area as well as the blade width are smaller in comparison with hydrofoil impellers. Radial outflow from the impeller C6 is substantially smaller and axial flow is predominant. Liquid flow returning from AH-B into the main flow is less pronounced. The upward axial flow along the baffle is not much suppressed and the suspension is better distributed throughout the entire vessel volume. Thus with the C6 impeller, the state of complete suspension occurs at lower impeller speeds with AH-B.

In the vessel with AH-B, the impellers C6 and LNC achieved approximately equivalent values of *Fr′*; the values were about 15 % higher for the impeller TXC, owing to its substantially lower *Po* value, see Fig. 5.

Overall, it can be said that AH-B was found to have a small effect on the *Fr′* values for impellers with smaller diameter (D/d = 3). Smaller impellers

T a b l e 3 – *Coefficients in Eq. (1) for the calculated functions Fr′ = f (d$_p$/D; φ) in the vessel with standard baffles (ST-B), H$_2$/d = 1*

Impeller symbol	D/d	C_{41}	C_{42}	a_1	a_2	C_{31}	C_{32}	c_1	c_2
B6	3	8.442	51.951	0.455	5.671	5.293	44.607	0.270	5.766
C6	2.5	5.302	54.012	0.443	5.728	3.879	55.552	0.210	7.592
TXB	3	18.623	20.002	0.507	1.840	5.786	18.057	0.271	2.328
TXC	2.5	22.202	−3.706	0.537	−1.016	9.186	−5.994	0.294	−0.630
LNB	3	21.820	8.002	0.577	0.344	2.202	23.214	0.111	3.434
LNC	2.5	5.399	7.404	0.414	0.285	1.804	0.629	0.075	0.082

T a b l e 4 – *Coefficients in Eq. (1) for the calculated functions* $Fr' = f(d_p/D; \varphi)$ *in the vessel with arrow-headed baffles (AH-B),* $H_z/d = 1$.

Impeller symbol	D/d	C_{41}	C_{42}	a_1	a_2	C_{31}	C_{32}	c_1	c_2
B6	3	26.741	23.669	0.604	2.120	5.364	24.760	0.230	3.596
C6	2.5	4.786	29.264	0.422	2.792	3.371	19.884	0.185	2.724
TXB	3	9.282	28.254	0.413	2.984	1.201	34.847	0.033	4.928
TXC	2.5	16.260	8.916	0.488	0.668	3.714	8.766	0.176	1.452
LNB	3	20.655	11.028	0.569	0.788	0.670	47.794	−0.077	7.430
LNC	2.5	6.428	17.639	0.450	1.433	1.756	24.690	0.068	4.027

attain higher critical impeller speeds than larger ones, and the lowest critical speeds, n_{cr}, were achieved with impeller LNB, followed by impeller B6. The highest n_{cr} values were reached with the impeller TXB. The latter finding is valid for both baffling types. For larger impellers (D/d = 2.5), the effect of AH-B is more noticeable. AH-B was found to have a positive effect on the Fr' values in case of the six pitched blade impeller C6, whereas the opposite was true with hydrofoil impellers TXC and LNC. In the vessel with ST-B, the lowest particle lifting speeds, n_{cr}, were attained with impeller LNC, followed by impellers C6 and TXC.

Effects of arrow-headed baffles on the impeller suspension efficiency π_S

Having ascertained the power numbers Po, as shown in Table 2, and the suspension characteristics $Fr' = f(d_p/D; \varphi)$, it is possible by means of Eq. (2) to calculate the suspension characteristics $\pi_S = f(d_p/D; \varphi)$, and then the volumetric impeller power $P_m = f(d_p/D; \varphi)$ from Eq. (3).

The effects of these two types of baffles and the comparisons thereof, from the point of view of energy savings, are illustrated in Fig. 7, where the functions $\pi_S = f(d_p/D; \varphi)$ are plotted. The shapes of these curves are analogous to those of the functions $Fr' = f(d_p/D; \varphi)$, but the curves are shifted by a constant which is a function of the power number Po, impeller diameter d, and vessel diameter D.

With smaller impellers (B6, LNB, TXB with D/d = 3), the arrow-headed baffles decrease the π_S values for all the impellers. An example of this behaviour is shown in Fig. 7a for the impeller B6 which yielded the largest decrease of π_S. At the same time, the respective π_S values obtained, under comparable conditions, with the hydrofoil impellers LNB and TXB are systematically lower than those obtained with B6. Hydrofoil impellers of this type and size are most favourable in terms of energy savings. It should be noted, that this conclusion applies to both baffle types.

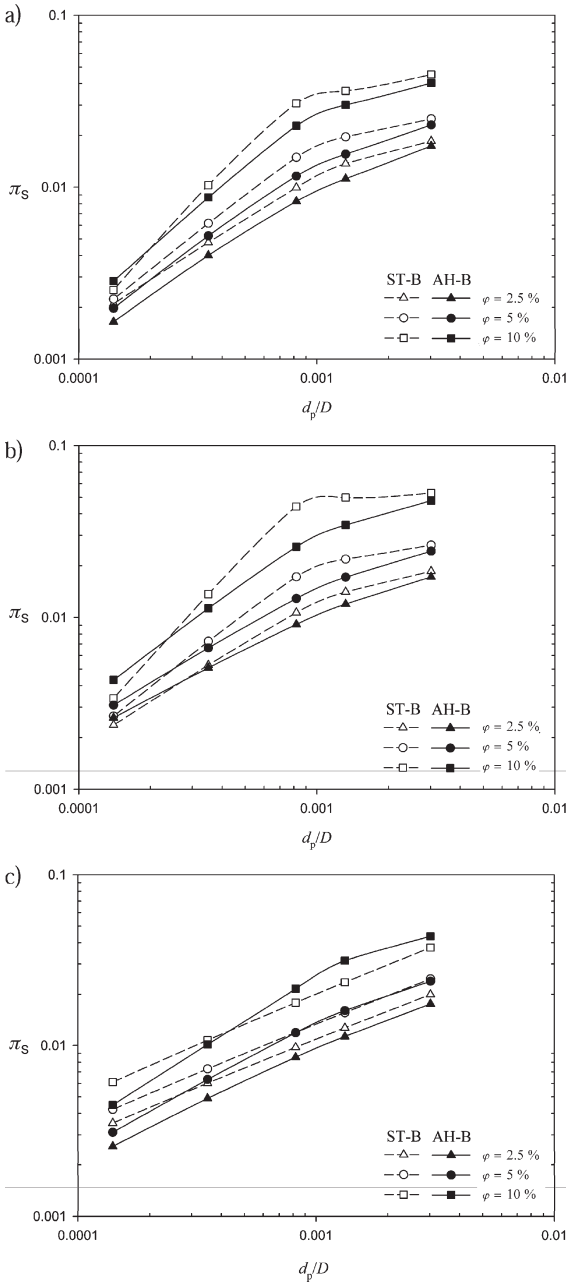

F i g . 7 – *Comparison of the functions* $\pi_S = f(d_p/D; \varphi)$ *for AH-B and ST-B: a) impeller B6, b) impeller C6, and c) impeller LNC*

With the larger impellers (C6, LNC, TXC with $D/d = 2.5$), the advantage of using AH-B is not so explicit as with smaller ones, as depicted in Figs. 7b and 7c. The arrow-headed baffles are energetically more advantageous, when using impeller C6 in suspensions of relative particle sizes $d_p/D > 2 \times 10^{-4}$. The hydrofoil impeller Lightnin A315 of a larger diameter d = 0.4 m gives better characteristics with the standard baffles in the regions $d_p/D > 3.5 \times 10^{-4}$ and $\varphi > 5$ %, as shown in Fig. 7c. For the larger hydrofoil impeller Techmix 335 in the region of $d_p/D < 7 \times 10^{-4}$, the arrow-headed baffles are preferable, whereas in the region of $d_p/D > 7 \times 10^{-4}$, a lower energy consumption is achieved with the standard baffles.

Effects of arrow-headed baffles on the volumetric impeller power P_m

In case of the dimensional quantity P_m, the discussion of comparisons of the baffle type effects for individual impellers is analogous to that which applied to the case of the dimensionless suspension efficiency π_S, because according to Eq. (3) and definition $P_m \equiv P/V$, the function $P_m = f(d_p/D; \varphi)$ is only a displacement of the function $\pi_S = f(d_p/D; \varphi)$, shifted by the factor $V^{-1}\rho_S\,[(\rho/g\,\Delta\rho)^3/\,D^7]^{-0.5}$ reflecting the physical properties of the suspension system. Calculated values of the volumetric impeller power $P_m = f(d_p/D; \varphi)$ under the just suspended conditions are presented in Table 5 for the solids concentration φ = 10 %, which could rather be expected in most industrial applications.

The following outcomes can be deduced from Table 5:

For the finest particles $d_p/D = 1.4 \times 10^{-4}$, the effect of baffle type on the values of P_m is relatively insignificant when using smaller impellers. Nevertheless, the trends of the suspension characteristics Fr', π_S, $P_m = f(d_p/D; \varphi)$ deserve to be investigated more comprehensively in the region of relative particle sizes $d_p/D \leq 1.4 \times 10^{-4}$.

Power consumption is greater for the larger impellers (D/d = 2.5) with either standard or arrow-headed baffles. The hydrofoil impellers, Lightnin A315 and Techmix 335 (D/d = 2.5 or 3), yield more substantial energy savings than the corresponding pitched blade impellers, and this conclusion applies to both baffle types. In these cases, the decrease of the P_m values ranges from 23 to 45 % and from 10 to 55 % for the smaller and for the larger impellers, respectively.

The mixing vessel that can be recommended for its minimum power consumption is stirred with the smaller hydrofoil impellers (D/d =3) Lightnin A315 or Techmix 335 in combination with arrow-headed baffles.

Conclusion

The arrow-headed baffles decrease the values of both, Po_0 and Po by approximately 12 % on the average, compared to the standard baffles. This systematic decrease indicates a better-ordered hydrodynamic flow pattern in the vessel with AH-B.

The suspension characteristics $Fr' = f(d_p/D; \varphi)$ and $\pi_S = f(d_p/D; \varphi)$ were established, making it possible to assess quantitatively the impeller sus-

Table 5 – *Values of the volumetric impeller power P_m for solids loading φ = 10 vol. %*

φ = 10 %			P_m/kW m^{-3}					
impeller symbol			B6	LNB	TXB	C6	LNC	TXC
D/d				3			2.5	
standard baffles	d_p/D	0.00014	0.20	0.28	0.24	0.27	0.49	0.51
		0.00035	0.85	0.65	0.63	1.13	0.89	0.94
		0.00082	2.65	1.43	1.45	3.81	1.54	1.59
		0.00132	3.03	1.83	1.78	4.15	1.95	1.90
		0.00302	3.86	2.38	2.33	4.51	3.19	2.62
arrow-headed baffles	d_p/D	0.00014	0.23	0.21	0.19	0.35	0.36	0.38
		0.00035	0.72	0.52	0.53	0.93	0.84	0.83
		0.00082	1.96	1.24	1.28	2.22	1.85	1.67
		0.00132	2.50	1.77	1.63	2.87	2.61	2.15
		0.00302	3.44	2.03	2.15	4.08	3.72	3.13

pension efficiency either from the aspect of the critical speeds required, n_{cr}, or from the aspect of the required power, P_m.

In comparison with the standard baffles, the arrow-headed baffling decreases the Fr' values somewhat for all the smaller impellers ($D/d = 3$) and also for the larger pitched-blade impeller C6 ($D/d = 2.5$), but a remarkable increase of these values was noted for the larger hydrofoil impellers.

In terms of potential energy savings, the non-standard vessel baffling is of advantage for achieving a complete off-bottom lifting of the particles, if combined with impellers of a smaller diameter ($D/d = 3$ – B6, LNB, TXB), or with the impeller C6 of a larger diameter ($D/d = 2.5$). With hydrofoil impellers LNC and TXC of a larger diameter ($D/d = 2.5$), the energy effectiveness of AH-B depends not only on the relative particle sizes, d_p/D, but also on the solids fraction, φ. Therefore, these impellers cannot be recommended for universal applications in suspension mixing processes.

The mixing vessel that can be recommended for its minimum power consumption is stirred with the smaller hydrofoil impellers ($D/d = 3$) Lightnin A315 or Techmix 335 in combination with arrow-headed baffles.

ACKNOWLEDGEMENT

The support of the Czech Ministry of Education under the MSM 6046137306 project is gratefully acknowledged.

Symbols

b – baffle width, m
D – vessel diameter, m
d – impeller diameter, m
d_p – particle diameter, m
Fr' – modified Froude number, $Fr' = n_{cr}^2\, d\rho/(\Delta\rho g)$
g – acceleration at gravity, m s^{-2}
H – filling height, m
H_2 – impeller off-bottom clearance, m
h – blade width, m
N_B – number of blades
M – shaft torque, N m
n – impeller speed, s^{-1}
n_{cr} – critical impeller speed, s^{-1}
P – impeller power consumption in suspension, W
P_m – volumetric impeller power at n_{cr}, W m^{-3}
P_w – impeller power consumption in water, W
Po – power number in suspension, $Po = P/(\rho_S\, n_{cr}^3\, d^5)$
Po_0 – power number in water, $Po_0 = P_w/(\rho\, n^3\, d^5)$
q_N – flow number
V – vessel volume, m^3

Greek letters

α – angle of blade
η – dynamic viscosity, Pa s
π_S – impeller suspension efficiency
ρ – liquid density, kg m^{-3}
ρ_p – solids density, kg m^{-3}
ρ_s – suspension density, kg m^{-3}
$\Delta\rho$ – solid-liquid density difference, $\Delta\rho = \rho_p - \rho$, kg m^{-3}
φ – solids volume fraction, %

References

1. *Zwietering, Th.N.,* Chem. Eng. Sci. **8** (1958) 244.
2. *Nienow, A.W.,* Chem. Eng. Sci. **23** (1968) 1453.
3. *Chudacek, M.W.,* Ind. Eng. Chem. Fundam. **25** (1986) 391.
4. *Ibrahim, S., Nienow, A.W.,* Trans.IChemE. **74/A** (1996) 679.
5. *Borowski, J., Wesolowski, P.,* Proc. of 12th Internat. Congress CHISA, Prague, Czech Republic (1996) P 7.24, pp. 1–10.
6. *Murugesan, T.*, J. Chem. Eng. Japan **34** (2001) 423.
7. *Wu, J., Zhu, Y.G., Pullum, L.,* AICHE Journal **48** (2002) 1349.
8. *Geisler, R.K., Buurman, C., Mersmann, A.B.,* Chem. Eng. J. **51** (1993) 29.
9. *Myers, K.J., Reeder, M.F., Fasano, J.B.,* Chem. Eng. Progress **98(2)** (2002) 42.
10. *Heywood, N.I., Rehman, S., Whittemore, R.G.,* Proc. of 7th Eur. Conf. on Mixing, (1991) pp. 469–482.
11. *Strenk, F., Karcz, J.,* Chem. Eng. Process. **32** (1993) 349.
12. *Karcz, J., Więch, D.,* Proc. of 15th Internat. Congress CHISA, Prague, Czech Republic (2002) P 5.161, pp. 1–8.
13. *Myers, K.J., Fasano, J.B.,* Can. J. Chem. Eng. **70** (1992) 596.
14. *Karcz, J., Major, M.,* Proc. of 13th Internat. Congress CHISA, Prague, Czech Republic (1998) P 1.30, pp. 1–9.
15. *Karcz, J., Major, M.,* Proc. of 11th Czech Conf. on Mixing, Brno, Czech Republic (1997) pp. 1–10.
16. *Medek, J., Seichter, P.,* Proc. of 48th National Conf. CHISA, Srní, Czech Republic (2001) B 4.1, pp. 1–4, in Czech.
17. *Raghava Rao, K.S.M.S., Rewatkar, V.B., Joshi, J.B.,* AICHE J. **34(8)** (1988) 1332.
18. *Sinevič, V.,* Proc. of 11th Internat. Congress CHISA, Prague, Czech Republic (1993) H3.128, pp. 1–11.
19. *Rieger, F., Ditl, P.,* Chem. Eng. Sci. **49** (1994) 2219.
20. *Rieger, F.,* Reports of the Faculty of Chem. and Process Eng. at the Warsaw University of Technology, Vol. **XXV**, No 1–3 (1999) 211.
21. *Rieger, F.*, Chem. Eng. J. **79** (2000) 171.
22. *Rieger, F.,* Chem. Eng. Process **41** (2002) 381.
23. *Rieger, F., Jirout, T., Ditl, P., Kysela, B., Sperling, R., Jembere, S.,* Proc. of 11th Eur. Conf. on Mixing, (2003) pp. 503–509.
24. *Rieger, F.,* Proc. of 6th Polish Seminar on Mixing. Technical University of Cracow, (1993) pp. 79–85.
25. *Špidla, M., Sinevič, V.,* Proc. of 13th Czech Conf. on Mixing, Brno, Czech Republic (2003) pp. 1–11, in Czech.
26. *Špidla, M., Sinevič, V., Hnízdil, T.,* Proc. of 50th National Conf. CHISA, Srní, Czech Republic (2003) B 5.5, pp. 1–12, in Czech.